

## Supporting Information for

### Stabilizing non-IPR $C_2(13333)-C_{74}$ cage with $Lu_2C_2/Lu_2O$ : the importance of encaged non-metal elements

Pengwei Yu,<sup>‡a</sup> Mengyang Li,<sup>‡b</sup> Shuaifeng Hu,<sup>a</sup> Changwang Pan,<sup>a</sup> Wangqiang Shen,<sup>a</sup> Kun Guo,<sup>a</sup> Yun-Peng Xie,<sup>a</sup> Lipiao Bao,<sup>\*a</sup> Rui Zhang,<sup>\*c</sup> and Xing Lu<sup>\*a,e</sup>

<sup>a</sup> *State Key Laboratory of Materials Processing and Die & Mould Technology, School of Materials Science and Engineering, Huazhong University of Science and Technology, 1037 Luoyu Road, Wuhan, 430074 China. E-mail: [baol@hust.edu.cn](mailto:baol@hust.edu.cn), [lux@hust.edu.cn](mailto:lux@hust.edu.cn)*

<sup>b</sup> *School of Physics, Xidian University, Xi'an, 710071 China.*

<sup>c</sup> *Key Laboratory for Green Chemical Process of Ministry of Education, School of Chemical Engineering and Pharmacy, Wuhan Institute of Technology, Wuhan 430205, China. E-mail: [ruizhang@wit.edu.cn](mailto:ruizhang@wit.edu.cn)*

<sup>d</sup> *School of Chemistry and Chemical Engineering, Jinggangshan University, Ji'an 331000, China.*

<sup>e</sup> *College of Chemistry and Chemical Engineering, Hainan University, No. 58, Renmin Avenue, Haikou 570228, China*

<sup>‡</sup> These authors contributed equally.

## Table of Contents

### Experimental.

**Figure S1.** Isolation of  $\text{Lu}_2\text{C}_2@C_2(13333)\text{-C}_{74}$  and  $\text{Lu}_2\text{O}@C_2(13333)\text{-C}_{74}$ .

**Figure S2.** HPLC chromatograms and LDI-TOF mass spectra of  $\text{Lu}_2\text{C}_2@C_2(13333)\text{-C}_{74}$  and  $\text{Lu}_2\text{O}@C_2(13333)\text{-C}_{74}$ .

**Table S1.** Crystallographic data of  $\text{Lu}_2\text{C}_2@C_2(13333)\text{-C}_{74}\cdot\text{Ni}^{\text{II}}(\text{OEP})\cdot 2(\text{C}_6\text{H}_6)\cdot\text{CS}_2$  and  $\text{Lu}_2\text{O}@C_2(13333)\text{-C}_{74}\cdot\text{Ni}^{\text{II}}(\text{OEP})\cdot 2(\text{C}_6\text{H}_6)\cdot\text{CS}_2$ .

**Figure S3.** Packing structures of  $\text{Lu}_2\text{C}_2@C_2(13333)\text{-C}_{74}\cdot\text{Ni}^{\text{II}}(\text{OEP})\cdot 2(\text{C}_6\text{H}_6)\cdot\text{CS}_2$  and  $\text{Lu}_2\text{O}@C_2(13333)\text{-C}_{74}\cdot\text{Ni}^{\text{II}}(\text{OEP})\cdot 2(\text{C}_6\text{H}_6)\cdot\text{CS}_2$ .

**Figure S4.** Positions of the disordered metal atoms in  $\text{Lu}_2\text{C}_2@C_2(13333)\text{-C}_{74}$  and  $\text{Lu}_2\text{O}@C_2(13333)\text{-C}_{74}$ .

**Table S2.** The fractional occupancies of the metal positions in  $\text{Lu}_2\text{C}_2@C_2(13333)\text{-C}_{74}$  and  $\text{Lu}_2\text{O}@C_2(13333)\text{-C}_{74}$ .

**Figure S5.** Structures of the major Lu metal sites with respect to the neighboring fused pentagons in (a)  $\text{Lu}_2\text{C}_2@C_2(13333)\text{-C}_{74}$  and (b)  $\text{Lu}_2\text{O}@C_2(13333)\text{-C}_{74}$ .

**Figure S6.** Vis-NIR absorption spectra of  $\text{Lu}_2\text{C}_2@C_2(13333)\text{-C}_{74}$  and  $\text{Lu}_2\text{O}@C_2(13333)\text{-C}_{74}$ .

**Table S3.** Characteristic absorption data of  $\text{Lu}_2\text{C}_2@C_2(13333)\text{-C}_{74}$  and  $\text{Lu}_2\text{O}@C_2(13333)\text{-C}_{74}$ .

## Experimental

### Preparation

The core-drilled graphite rods filled with a homogeneous mixture of graphite powder and  $\text{Lu}_2\text{O}_3$  (molar ratio of M/C = 1:17) were annealed in a tube furnace at 1000 °C for 12 hours under argon atmosphere. The rods were then vaporized in a Krätschmer-Huffman-type fullerene generator with an arc current of 100 A under a mixture of 270 Torr helium and 15 Torr  $\text{CO}_2$  atmospheres. The as-produced fullerene soot was collected and sonicated in carbon disulfide for 1h. After filtration,  $\text{CS}_2$  was removed using a rotary evaporator. The solid residue was dissolved in toluene and filtered.

### High-performance Liquid Chromatography (HPLC) Separation Processes

$\text{Lu}_2\text{C}_2@C_2(13333)\text{-C}_{74}$  and  $\text{Lu}_2\text{O}@C_2(13333)\text{-C}_{74}$  were isolated by a multiple-stage HPLC process using toluene as eluent. The first stage was performed on a Buckyprep column (20 mm × 250 mm, Cosmosil Nacalai Tesque), and a fraction named as Fr5 was collected (Fig. S1a). Then, Fr5 was injected into a Buckyprep-M column (20 mm × 250 mm, Cosmosil Nacalai Tesque) for the second stage separation, and a fraction named as Fr5-2 was obtained (Fig. S1b). Fr5-2 was injected into a Buckyprep column (20 mm × 250 mm, Cosmosil Nacalai Tesque), and a fraction named as Fr5-2-3 was collected (Fig. S1c). As for Fr5-2-3, a 5PYE column (20 mm × 250 mm, Cosmosil Nacalai Tesque) was used for the separation, and a fraction named as Fr5-2-3-1 was obtained (Fig. S1d). After that, Fr5-2-3-1 was injected a Buckyprep-M column (10 mm × 250 mm, Cosmosil Nacalai Tesque), and a fraction named as Fr5-2-3-1-1 was collected along with pure  $\text{Lu}_2\text{C}_2@C_2(13333)\text{-C}_{74}$  (Fr5-2-3-1-3) was obtained (Fig. S1e). As for Fr5-2-3-1-1, a Buckyprep column (20 mm × 250 mm, Cosmosil Nacalai Tesque) was used for the last stage separation, and pure  $\text{Lu}_2\text{O}@C_2(13333)\text{-C}_{74}$  was finally obtained (Fig. S1f).

### Spectroscopic and electrochemical studies

LDI-TOF mass spectrometry was conducted on a BIFLEX III spectrometer (Bruker Daltonics Inc., Germany). Vis-NIR spectra were measured on a Lambda 35 spectrophotometer (PerkinElmer, USA) in  $\text{CS}_2$ . CV curves were obtained in *o*-

dichlorobenzene with 0.05 M TBAPF<sub>6</sub> as electrolyte using a CHI-660E instrument.

### **Crystallographic characterizations**

Crystalline blocks of Lu<sub>2</sub>C<sub>2</sub>@C<sub>2</sub>(13333)-C<sub>74</sub> and Lu<sub>2</sub>O@C<sub>2</sub>(13333)-C<sub>74</sub> were obtained by layering a benzene solution of Ni<sup>III</sup>(OEP) over a carbon disulfide solution of the endohedral in a glass tube, respectively. Single-crystal XRD measurements were performed at 100 K using synchrotron radiation ( $\lambda = 0.71073 \text{ \AA}$ ) with a MarCCD detector at beamline BL17B station of Shanghai Synchrotron Radiation Facility. The multiscan method was used for absorption corrections. The structures were solved by direct method and were refined with SHELXL-2014. Hydrogen atoms were inserted at calculated positions and constrained with isotropic thermal parameters. Details of crystal data are listed in ESI. These data can be obtained free of charge from The Cambridge Crystallographic Data Centre with CCDC Nos. 2268031 and 2268032.

### **Computational studies**

The optimizations of Lu<sub>2</sub>C<sub>2</sub>@C<sub>2</sub>(13333)-C<sub>74</sub> and Lu<sub>2</sub>O@C<sub>2</sub>(13333)-C<sub>74</sub> were carried out on the PBE0/6-31G(d)-SDD level without any imaginary frequency, where 6-31G(d) was for carbon and oxygen atoms and SDD with pseudopotential was for lutetium atoms. All of the above calculations were performed with Gaussian 16 software except for the specific illustration.

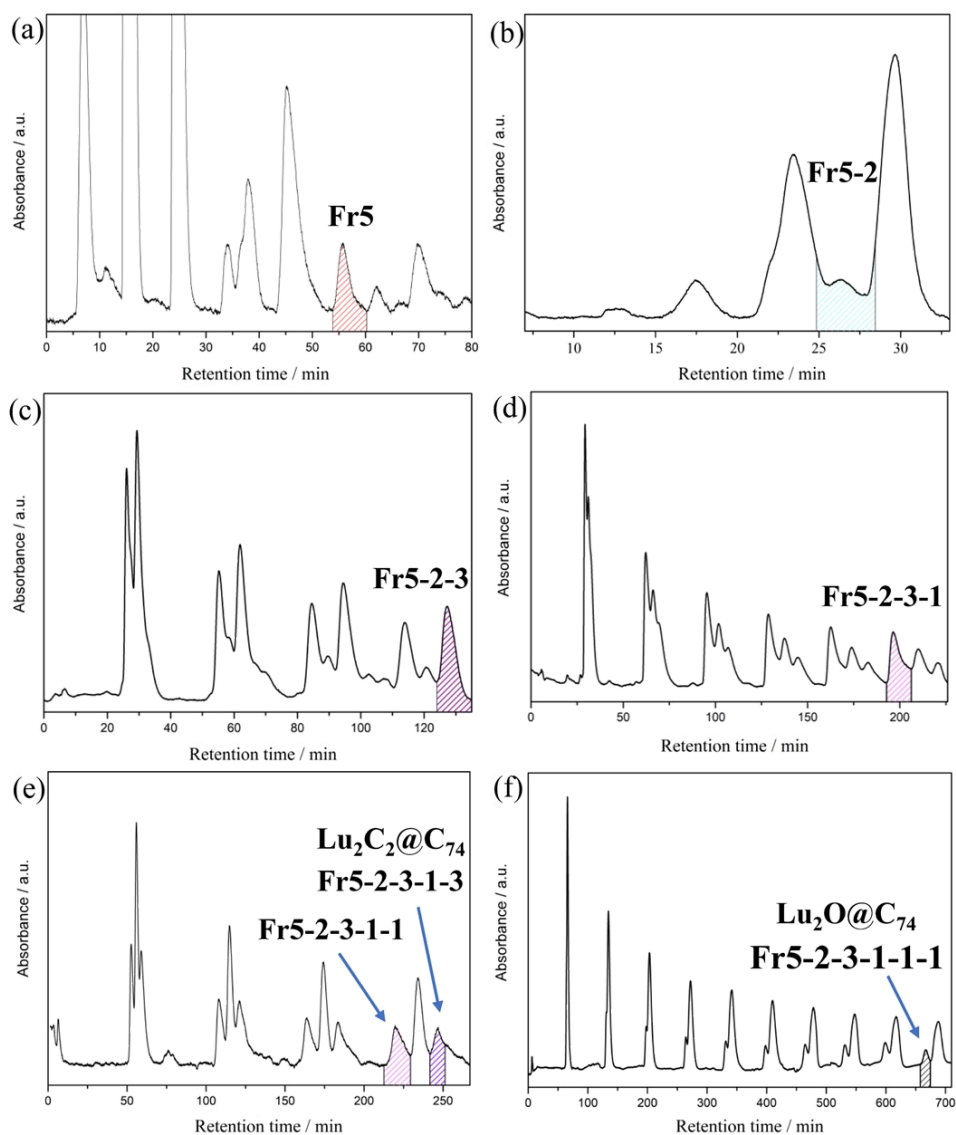


**Figure S1.** Isolation schemes of  $\text{Lu}_2\text{C}_2@\text{C}_2(13333)\text{-C}_{74}$  and  $\text{Lu}_2\text{O}@\text{C}_2(13333)\text{-C}_{74}$ . (a) HPLC profile of soot extract containing Lu-based metallofullerene on a Buckyprep column. Conditions: 20 mL injection volume; 10 mL/min toluene flow. (b) HPLC chromatogram of Fr5 on a Buckyprep-M column. Conditions: 20 mL injection volume; 10 mL/min toluene flow. (c) Recycling HPLC profile of Fr5-2 on a Buckyprep column. Conditions: 15 mL injection volume; 10 mL/min toluene flow. (d) Recycling HPLC profile of Fr5-2-3 on a 5PYE column. Conditions: 10 mL injection volume; 10 mL/min toluene flow. (e) Recycling HPLC profile of Fr5-2-3-1 on a Buckyprep-M column. Conditions: 10 mL injection volume; 10 mL/min toluene flow. (f) Recycling HPLC profile of Fr5-2-3-1-1 on a Buckyprep column. Conditions: 10 mL injection volume; 10 mL/min toluene flow. (All of the detection wavelengths are 330 nm.)

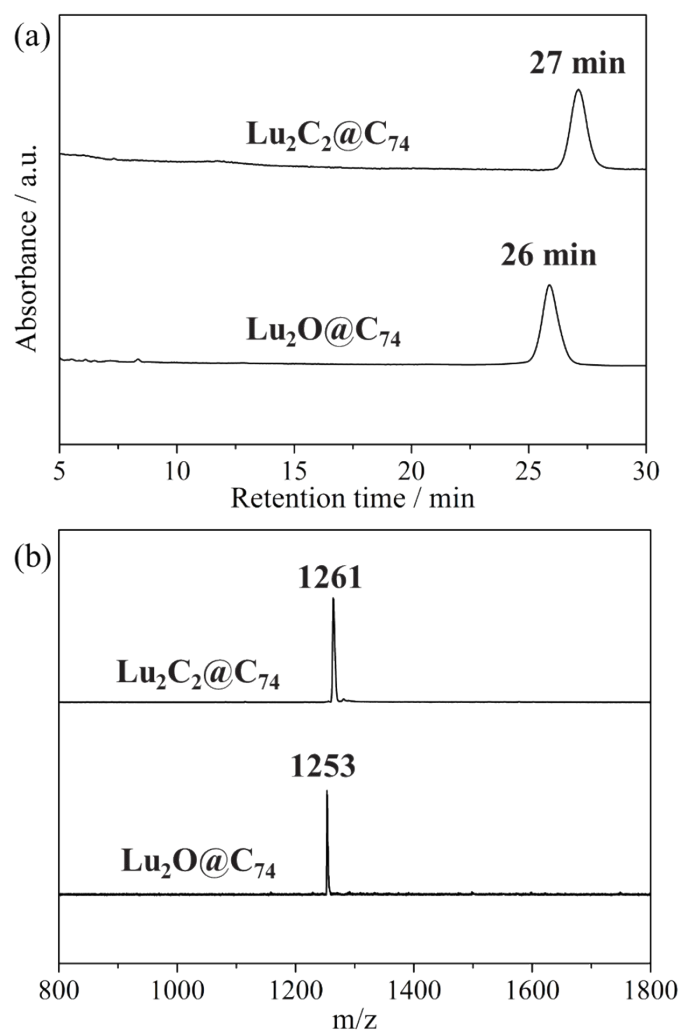


**Figure S2.** (a) HPLC chromatograms and (b) LDI-TOF mass spectra of  $\text{Lu}_2\text{C}_2@\text{C}_{74}$  and  $\text{Lu}_2\text{O}@\text{C}_{74}$ . HPLC conditions: Buckyprep column ( $\phi = 4.6 \times 250$  mm); 20  $\mu\text{L}$  injection volume; 1  $\text{mL min}^{-1}$  toluene flow; 330 nm detection wavelength; 40  $^\circ\text{C}$ .

**Table S1.** Crystallographic data of  $\text{Lu}_2\text{C}_2@C_2(13333)-C_{74}\cdot\text{Ni}^{\text{II}}(\text{OEP})\cdot 2(\text{C}_6\text{H}_6)\cdot\text{CS}_2$  and  $\text{Lu}_2\text{O}@C_2(13333)-C_{74}\cdot\text{Ni}^{\text{II}}(\text{OEP})\cdot 2(\text{C}_6\text{H}_6)\cdot\text{CS}_2$ .

	$\text{Lu}_2\text{C}_2@C_2(13333)-C_{74}\cdot\text{Ni}^{\text{II}}(\text{OEP})\cdot 2(\text{C}_6\text{H}_6)\cdot\text{CS}_2$	$\text{Lu}_2\text{O}@C_2(13333)-C_{74}\cdot\text{Ni}^{\text{II}}(\text{OEP})\cdot 2(\text{C}_6\text{H}_6)\cdot\text{CS}_2$
<b><i>T</i>, K</b>	100(2)	100(2)
<b><math>\lambda</math>, Å</b>	0.71073	0.71073
<b>color/habit</b>	black/block	black/block
<b>cryst size, mm</b>	0.08×0.06×0.04	0.08×0.06×0.06
<b>empirical formula</b>	$\text{C}_{244}\text{H}_{106}\text{Lu}_4\text{N}_8\text{S}_4\text{Ni}_2$	$\text{C}_{240}\text{H}_{106}\text{Lu}_4\text{N}_8\text{S}_4\text{Ni}_2\text{O}_2$
<b>fw</b>	4094.90	4078.79
<b>cryst system</b>	monoclinic	monoclinic
<b>space group</b>	<i>C2/m</i>	<i>C2/m</i>
<b><i>a</i>, Å</b>	25.898(3)	25.811(3)
<b><i>b</i>, Å</b>	16.702(2)	16.724(2)
<b><i>c</i>, Å</b>	17.940(2)	17.817(2)
<b><math>\alpha</math>, deg</b>	90	90
<b><math>\beta</math>, deg</b>	106.615(4)	106.529(4)
<b><math>\gamma</math>, deg</b>	90	90
<b><i>V</i>, Å<sup>3</sup></b>	7435.7(17)	7734.3(4)
<b><i>Z</i></b>	2	2
<b><math>\rho</math>, g/cm<sup>3</sup></b>	1.829	1.837
<b><math>\mu</math>, mm<sup>-1</sup></b>	3.010	3.036
<b><math>R_1</math> [<math>I &gt; 2\sigma(I)</math>]</b>	0.0724(5410)	0.0830(5268)
<b><math>wR_2</math> (all data)</b>	0.2404(6963)	0.2775(6953)

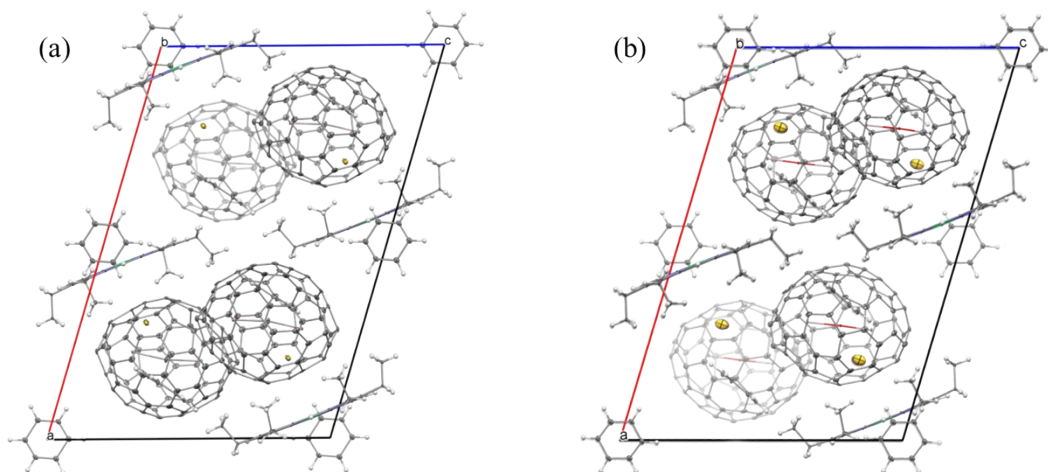


**Figure S3.** Packing structures of (a)  $\text{Lu}_2\text{C}_2@C_2(13333)\text{-C}_{74}\cdot\text{Ni}^{\text{II}}(\text{OEP})\cdot 2(\text{C}_6\text{H}_6)\cdot\text{CS}_2$  and (b)  $\text{Lu}_2\text{O}@C_2(13333)\text{-C}_{74}\cdot\text{Ni}^{\text{II}}(\text{OEP})\cdot 2(\text{C}_6\text{H}_6)\cdot\text{CS}_2$ .

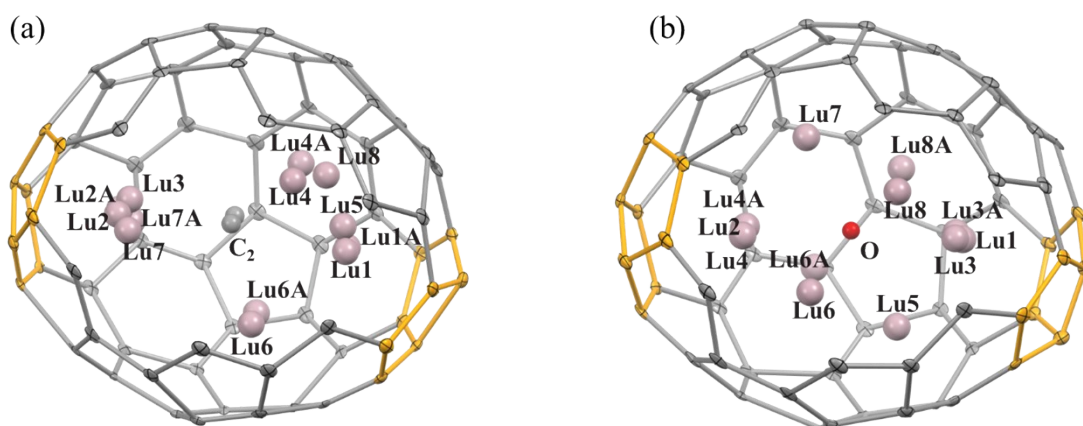


**Figure S4.** Positions of the disordered metal sites in (a)  $\text{Lu}_2\text{O}@C_s(6)\text{-C}_{82}$  and (b)  $\text{Er}_2\text{O}@C_s(6)\text{-C}_{82}$  relative to the cage orientation. The metal sites labeled with “A” are generated by crystallographic operation and a part of the cages are omitted for clarity.



**Table S2.** The fractional occupancies of the metal positions in  $\text{Lu}_2\text{O}@C_s(6)\text{-C}_{82}$  and  $\text{Er}_2\text{O}@C_s(6)\text{-C}_{82}$ .

Compounds	Fractional occupancy of the metal positions							
	Lu1/Lu1A	Lu2/Lu2A	Lu3	Lu4/Lu4A	Lu5	Lu6/Lu6A	Lu7/Lu7A	Lu8
$\text{Lu}_2\text{C}_2@C_2(13333)\text{-C}_{74}$	0.35	0.33	0.11	0.08	0.08	0.08	0.05	0.02
$\text{Lu}_2\text{O}@C_2(13333)\text{-C}_{74}$	0.31	0.50	0.22	0.12	0.09	0.07	0.05	0.10

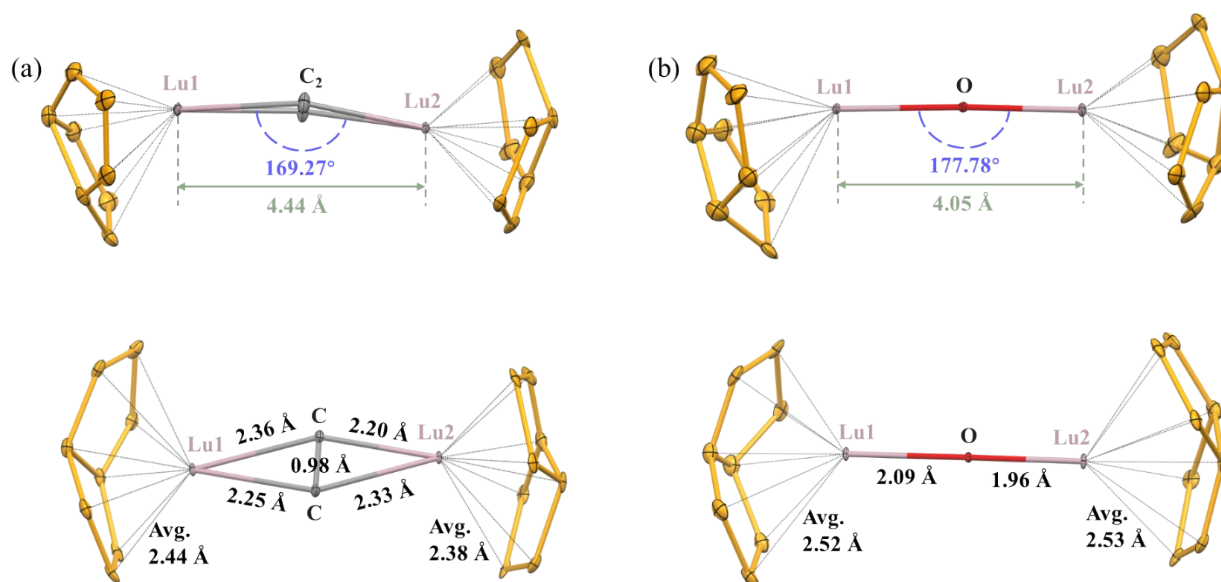


**Figure S5.** Structures of the major Lu metal sites with respect to the neighboring fused pentagons in (a)  $\text{Lu}_2\text{C}_2@C_2(13333)\text{-C}_{74}$  and (b)  $\text{Lu}_2\text{O}@C_2(13333)\text{-C}_{74}$ .

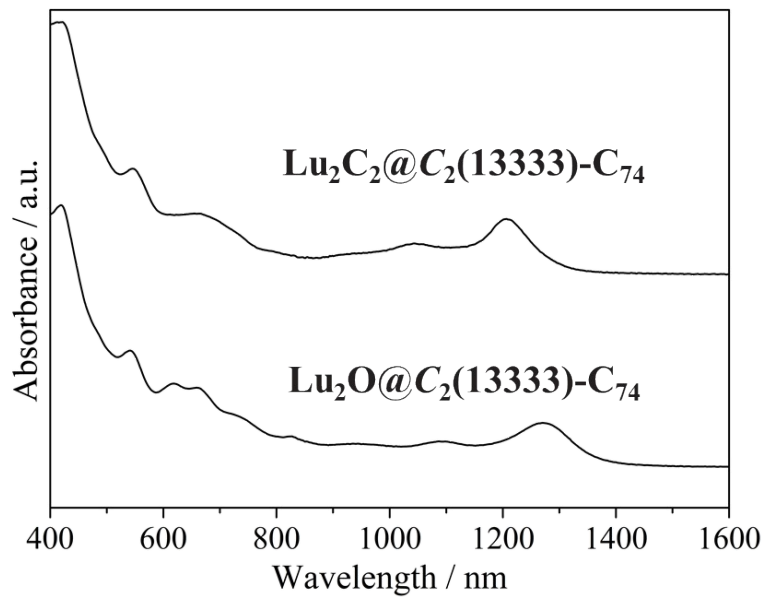


**Figure S6.** Vis-NIR absorption spectra of  $\text{Lu}_2\text{C}_2@\text{C}_2(13333)\text{-C}_{74}$  and  $\text{Lu}_2\text{O}@\text{C}_2(13333)\text{-C}_{74}$  dissolved in  $\text{CS}_2$  at room temperature.

**Table S3.** Characteristic absorption data of  $\text{Lu}_2\text{C}_2@\text{C}_2(13333)\text{-C}_{74}$  and  $\text{Lu}_2\text{O}@\text{C}_2(13333)\text{-C}_{74}$ .

Componds	Absorption peaks (nm)	Absorption onset ( $\lambda_{\text{onset}}$ , nm)	$\Delta E_{\text{gap, optical}} / \text{eV}^{\text{a}}$
$\text{Lu}_2\text{C}_2@\text{C}_2(13333)\text{-C}_{74}$	546, 667, 1042	1324	0.94
$\text{Lu}_2\text{O}@\text{C}_2(13333)\text{-C}_{74}$	542, 618, 663, 1089	1380	0.90

$$^{\text{a}}\Delta E_{\text{gap, optical}} = 1240/\lambda_{\text{onset}}$$